Study of K^+K^- production in π^+d interactions at 10 GeV/c, and evidence for a $J^P=7^-$ resonance $M(2750)$ decaying into $K^+K^-\pi^+$

D. L. Denney,* H. B. Crawley, A. Firestone, J. S. Hendrickson,† J. W. Lamsa, and W. T. Meyer
Department of Physics and Ames Laboratory, Iowa State University, Ames, Iowa 50011

J. W. Chapman and A. A. Seidl
Department of Physics, University of Michigan, Ann Arbor, Michigan 48109
(Received 9 May 1983)

We have studied the reactions $\pi^+n\to K^+K^-p$, $\pi^+p\to K^+K^-\Delta^{++}$, and $\pi^+p\to(K^+K^-\pi^+)p$ in 10-GeV/c π^+d interactions using the large-aperture solenoid spectrometer at SLAC. We measure the cross sections times branching ratios for the production of the known meson resonances $f(1270)$, $g(1690)$, and $h(2040)$. We also observe a new resonance with mass 2747±32 MeV, width 195±75 MeV, and production cross section times branching ratio into $K^+K^-\pi^+$ of 0.84±0.08 μb. The data are consistent with the quantum numbers of this state being $I=1$, $J^P=7^-$.

I. INTRODUTION

The development in recent years of particle detectors with nearly 4π acceptance and high-event-rate capabilities, such as the multiparticle spectrometer (MPS) at Brookhaven, the Omega Spectrometer at CERN, and the large-aperture solenoid spectrometer (LASS) and SLAC, has allowed the collection of large data samples which cover nearly the full angular distribution. In general, forward spectrometers can take high event rates but have limited angular acceptance, and bubble chambers have good angular acceptance but low event rates. The essential factors in the new spectrometers are the high statistics which allow for the determination of states produced with low cross section and the nearly complete geometrical acceptance, which is essential for a determination of the spin-parities of many states, especially when backgrounds are high.

This study is concerned with the reactions

$$\pi^+n\to K^+K^-p \tag{1}$$

and

$$\pi^+p\to K^+K^-\pi^+p\ . \tag{2}$$

By selecting the region of low four-momentum transfers from initial to final baryon we may isolate the virtual scattering reactions

$$\pi^+\pi^-\to K^+K^- \tag{3}$$

and

$$\pi^+\pi^0\to K^+K^-\pi^+\ , \tag{4}$$

although in the latter case we expect a large background from a Deck-type low-mass enhancement similar to that seen in 3π final states. We define t as the square of the four-momentum transfer from the initial baryon to the final baryon, so t is equal to the mass squared of the exchanged particle. The cross sections for reactions (1) and (2) in the low-t kinematic region are expected to be dominated by events with single-pion exchange, as this is the region closest to the pion pole.[1] For reactions (3) and (4), only those states of even-G parity can be produced at the meson vertex. Also, conservation of angular momentum and parity imply that only states with natural spin-parity are allowed, i.e., only states with $J^P=0^+,1^-,2^+$, etc., can be produced at the meson vertex.

The data described in this paper are part of an experiment which used the LASS facility at SLAC.[2] This exposure of the LASS detector resulted in approximately 11×10^6 events being recorded on magnetic tape, about 5.2×10^6 of which satisfied the primary physics trigger. These data were processed through computer programs for track reconstruction, geometrical fitting, and kinematic selection on the Iowa State University high-energy-physics Digital Equipment Corporation VAX 11/780 computer.

The data sample was corrected for the nonuniformity of the angular acceptance of the apparatus through the use of an intricate Monte Carlo simulation package for the generation of the acceptance-correction arrays. The data samples were then processed through an analysis routine which determined the acceptance-corrected mass and angular distributions as well as the spherical-harmonic moments of the angular distributions. A mass-dependent study of these moments was then performed.

In Sec. II the experimental apparatus and event trigger are briefly described. In Sec. III we present the principal data distributions, in Sec. IV we present the distributions in the acceptance-corrected angular moments, and in Sec. V we present the conclusions of this analysis.

II. EXPERIMENTAL APPARATUS AND EVENT TRIGGER

The experiment was performed by exposing the LASS detector to a 10-GeV/c π^+ beam incident on 1-m-long liquid-deuterium target. The LASS facility was used for this experiment because of its nearly complete 4π geome-

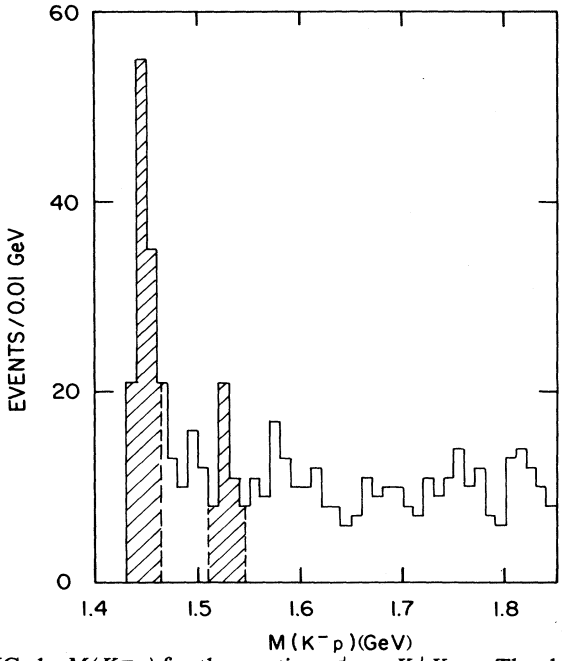

FIG. 1. $M(K^-p)$ for the reaction $\pi^+n \to K^+K^-p$. The shaded area indicates the region discarded. Note further that the bulk of the events are off-scale with $M(K^-p) > 1.8$ GeV.

trical acceptance as well as its good resolution in both transverse and longitudinal momenta. This apparatus is described in detail in the literature,[3-11] and a schematic drawing of the layout has been published in Ref. 3. The upstream superconducting solenoid magnet with an axial field allows a measurement of the momenta of particles with large-angle trajectories and relatively low momenta.

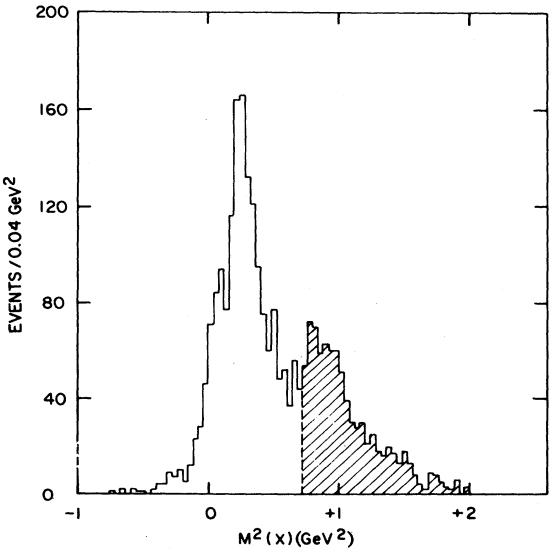

FIG. 2. $M^2(x)$ for the reaction $\pi^+n \to K^+K^-p$. The shaded area indicates the region discarded.

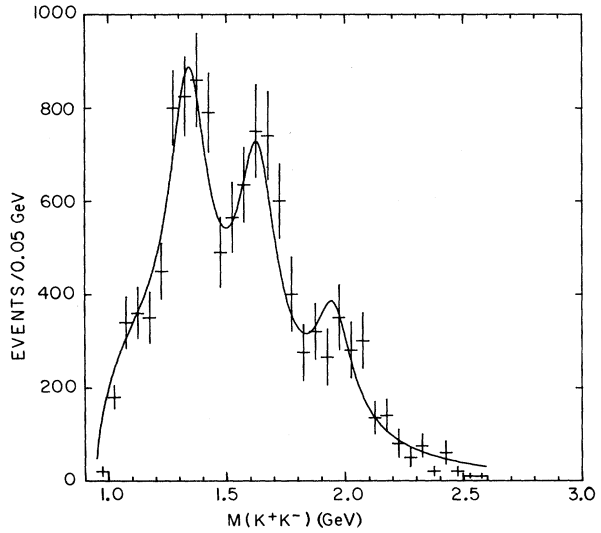

FIG. 3. Acceptance-corrected $M(K^+K^-)$ for the reaction $\pi^+n \to K^+K^-p$. The smooth curve shows the results of a fit described in the text.

The downstream dipole magnet with vertical field allows a measurement of the momenta of the small-angle high-momentum particles by joining track segments found in the chambers downstream of the dipole magnet to track segments found in the region between the two magnets via an extrapolation through the dipole field. Particle identification is accomplished with a time-of-flight scintillation counter array and two Cherenkov counters. The upstream

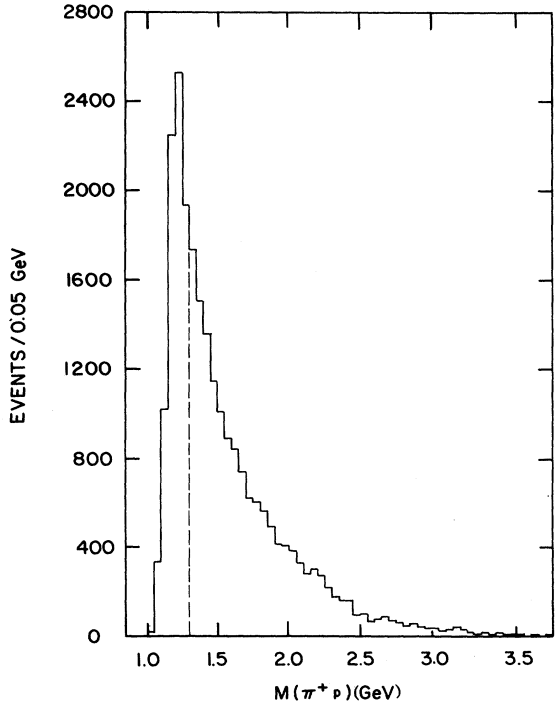

FIG. 4. $M(\pi^+p)$ for the reaction $\pi^+p \to K^+K^-\pi^+p$. The dashed line indicates the location of the cut described in the text.

TABLE I. K^+K^- resonances from $\pi^+n\to K^+K^-p$ and from $\pi^-p\to K^+K^-p$ data of Ref. 22.

Resonance	Width Γ (MeV)	Cross section $\times$ branching ratio into K^+K^- (μb)
	From $\pi^+n\to K^+K^-p$	
$f(1270)$	195±42	1.14±0.07
$g(1680)$	200±48	1.13±0.07
$h(2040)$	190±14	0.40±0.05
$\chi^2=32.3$ for 26 degrees of freedom		
	From $\pi^-p\to K^+K^-p$ $t'\leq 0.3$ GeV^2	
"g"	214±20	1.69±0.16
"h"	100±28	0.36±0.08
	$0.08<t'\leq 0.2$ GeV^2	
"g"	231±33	0.89±0.13
"h"	145^{+49}_{-34}	0.36±0.08

Cherenkov counter $C1$ is a 38-cell segmented counter located between the two magnets, and the downstream Cherenkov counter is an 8-cell counter located downstream of the last spark chamber.

The primary physics trigger in this experiment is designed to select events in which at least one of the particles produced in the forward direction is likely to be heavier than a pion, i.e., a kaon or proton. The trigger has five separate criteria: (1) A beam particle be detected and identified as a pion by two beam-line Cherenkov counters; (2) two or more hits be in the first planar proportional wire chamber; (3) no light be detected in the upstream segmented Cherenkov counter, which has a pion threshold of 3.0 GeV/c; (4) two or more hits be detected in the time-of-flight scintillation counter; and (5) one or more hits be detected in each of the three hodoscopes downstream of the dipole magnet. Since particles with momenta less than 3 GeV/c are deflected sufficiently by the dipole magnetic field that they do not cross the dipole aperture, this combination of requirements allows one to trigger the apparatus on events in which "fast" (>3 GeV/c) forward tracks are likely to be kaons or protons. The trigger rate for the primary physics trigger is 1.5%, and the total trigger rate for all triggers including various monitoring triggers is 3%.

III. EVENT SELECTION AND DATA DISTRIBUTIONS

Of the 11×10^6 events recorded on magnetic tape, approximately 5.2×10^6 events were from the primary physics trigger and were processed through track reconstruction, vertex finding, and geometry-fitting packages on the VAX 11/780 computer. This resulted in a data sample of 686 000 fully reconstructed events. Events were rejected because of unreconstructible trigger tracks (53% of losses), pion leakage into the trigger tracks due to poor efficiency of the upstream Cherenkov counter (45% of losses), and excessive background in the spark chambers (7% of losses). Inefficiency in some regions of the upstream Cherenkov counter (usually near cell boundaries) was so severe it necessitated rejection of all events with fast-forward particles passing through these regions as particle identification was too uncertain. For this study we select all three-prong and four-prong geometry-fitted events with missing longitudinal momentum less than 0.5 GeV/c, missing transverse momentum squared less than 0.02 (GeV/c)^2, and a net charge of $+1$ for the three prongs or $+2$ for the four prongs. These constraints select those events with final states of the correct charge and with no apparent missing momentum.

Further selection criteria for the three-prong K^+K^-p final-state events are as follows. (1) Identification for each of the individual particles be consistent with the hypothesis $\pi^+n\to K^+K^-p$, (2) the missing energy for the event be less than 0.3 GeV, (3) the square of the missing mass be less than 0.1 GeV^2, and (4) the square of the four-momentum transfer from the target nucleon to the recoil proton be less than 0.2 (GeV/c)^2. In the reaction $\pi^+n\to K^+K^-p$, one contribution to the background is the associated production reaction $\pi^+n\to K^+\Lambda^0(1520)$, with the strong decay $\Lambda(1520)\to K^-p$. There is also background due to the associated production reaction $\pi^+n\to K^+\Lambda^0(1115)$ in which the π^- from the weak decay $\Lambda^0\to\pi^-p$ is misidentified as a K meson. These two backgrounds are reduced by discarding events with $M(K^-p)<1.455$ GeV in order to eliminate the $\Lambda^0(1115)$ events, and discarding events with $1.510<M(K^-p)<1.535$ GeV in order to eliminate the $\Lambda^0(1520)$ events, as shown in Fig. 1. To further reduce the background due to misidentified pion and proton pairs we calculate the square of the invariant mass of the two particles forming the oppositely charged equal-mass pair $[M^2(x)]$. This variable is determined by scaling the longitudinal components of the momenta of the outgoing particles so that longitudinal momentum is exactly conserved, and then using conservation of energy. For the $K\bar{K}p$ data we observe an enhancement around the square of the proton mass, and this signal has been the subject of an analysis of the reaction $\pi^+n\to\bar{p}pp$.[12] There is no indication of a pion background. In order to select events of the reaction $\pi^+n\to K^+K^-p$ we require that $M^2(x)$ be less than 0.72 GeV^2, and this is shown in Fig. 2. We estimate

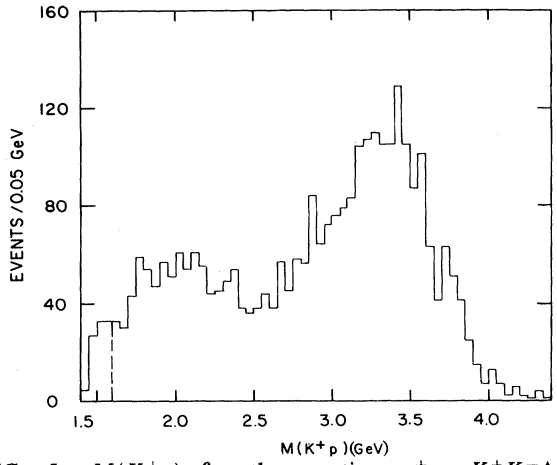

FIG. 5. $M(K^+p)$ for the reaction $\pi^+p \to K^+K^-\Delta^{++}$, $\Delta^{++} \to \pi^+p$. The dashed line indicates the location of the cut described in the text.

a contamination from $\bar{p}p$ events of 6%, and an upper limit on contamination from $\pi\pi$ events of 2%. The latter estimate is based on the small shoulder at $M^2(x) \approx 0$, which may be a residue of $\pi\pi$ events after the cuts on acceptable regions of $C1$ for trigger particles.

Those events surviving the above cuts are weighted for acceptance losses as determined by a Monte Carlo simulation package. The acceptance-corrected K^+K^- mass distribution for the $K\bar{K}p$ final state is shown in Fig. 3, in which a few mismeasured events with a calculated acceptance of less than 0.02 have been discarded. The solid curve on this graph represents a least-squares fit to the data of three Breit-Wigner resonance shapes plus a phase-space background. The three enhancements may be identified with the $f(1270)$, $g(1680)$, and $h(2040)$ resonances. The results of this fit are shown in Table I. There is no evidence for the production of any resonances other than these three known resonances. The cross sections quoted in Table I have been corrected for deuterium effects, specifically for the suppression due to the Pauli exclusion principle, which effects the very low-t region and is about 2% for the $\pi^+n \to K^+K^-p$ reaction. Also shown in Table I are cross-section results from the charge-symmetric reaction $\pi^-p \to K^+K^-n$ at 10 GeV/c, and the agreement is reasonable. For pure pseudoscalar exchange we expect similar cross sections for the two reactions.

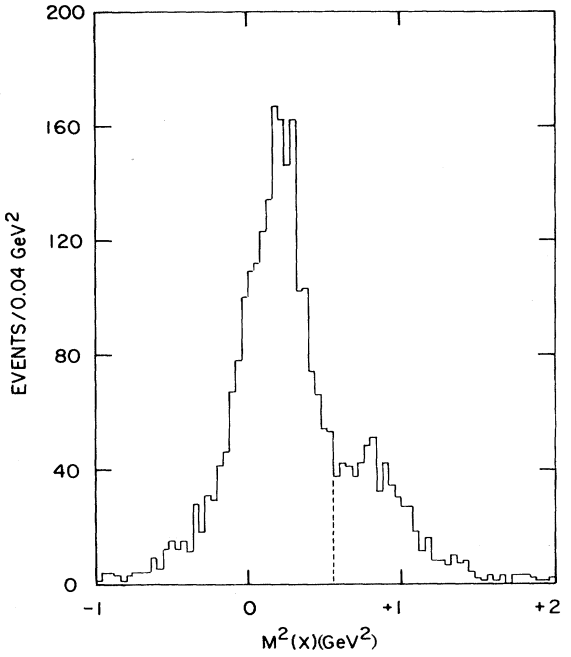

FIG. 7. $M^2(x)$ for the reaction $\pi^+p \to K^+K^-\Delta^{++}$. The dashed line indicates the location of the cut described in the text.

Further selection criteria for the four-prong $K^+K^-\pi^+p$ final-state events are as follows: (1) Identification for each of the individual particles be consistent with the hy-

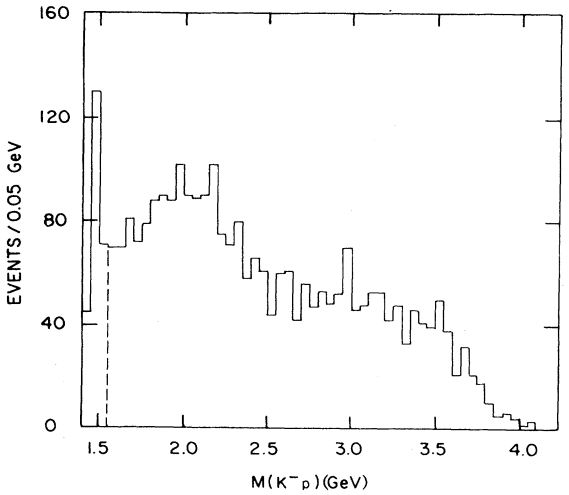

FIG. 6. $M(K^-p)$ for the reaction $\pi^+p \to K^+K^-\Delta^{++}$, $\Delta^{++} \to \pi^+p$. The dashed line indicates the location of the cut described in the text.

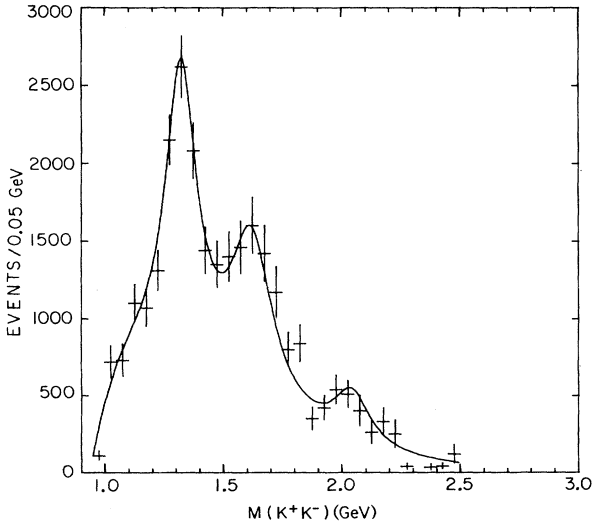

FIG. 8. Acceptance-corrected $M(K^+K^-)$ for the reaction $\pi^+p \to K^+K^-\Delta^{++}$. The smooth curve shows the results of a fit described in the text.

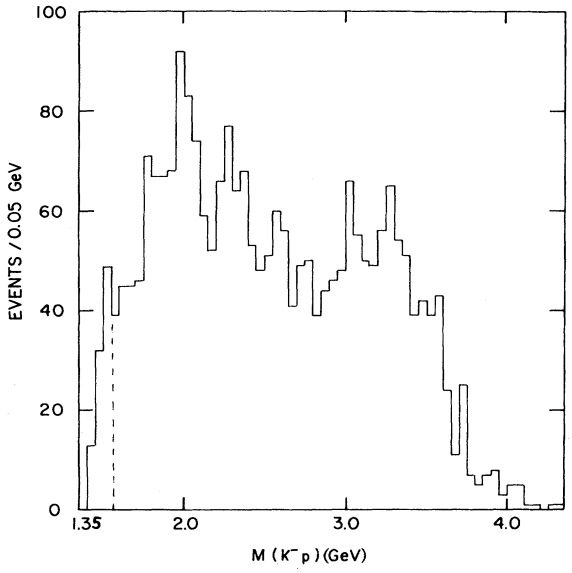

FIG. 9. $M(K^-p)$ for the reaction $\pi^+p\to K^+K^-\pi^+p$ (no Δ^{++}). The dashed line indicates the position of the cut.

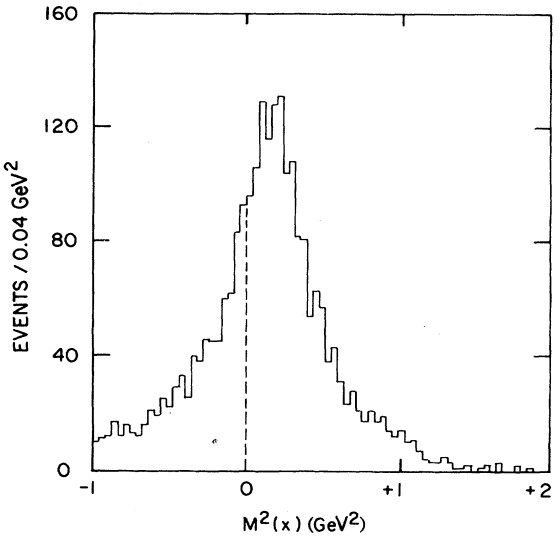

FIG. 11. $M^2(x)$ for the reaction $\pi^+p\to K^+K^-\pi^+p$ (no Δ^{++}). The dashed line indicates only the value $M^2(x)=0$.

pothesis $\pi^+p\to K^+K^-\pi^+p$; (2) the missing energy for the event be less than 0.3 GeV; (3) the square of the missing mass be less than 0.1 GeV^2; and (4) the square of the four-momentum transfer from the target nucleon to the recoil baryon be less than 0.5 (GeV/c)^2. In order to study the virtual scattering reaction $\pi^+\pi^-\to K^+K^-$ we select the Δ^{++} region of the π^+p mass distribution with the cut $M(\pi^+p)<1.35$ GeV, as shown in Fig. 4. The selection of the charge-exchange reaction at the baryon vertex ensures the absence of any $I=0$ exchange background to the $I=1$ exchange reaction studied. In the K^+p mass distribution we observe a small enhancement close to threshold. Monte Carlo simulations of the experiment indicate that this enhancement is a reflection of the Δ^{++}, where the π^+ from the decay $\Delta^{++}\to p\pi^+$ had been misidentified as a K^+. To eliminate this small background we require the K^+p mass to be greater than 1.60 GeV, as shown in Fig. 5. In the K^-p mass distribution we observe enhancements in the low-mass region due to the $\Lambda^0(1115)$ and $\Lambda^0(1520)$ states, similar to the π^+n reaction discussed earlier. We therefore require that the K^-p mass be greater than 1.55 GeV, as shown in Fig. 6. In order to further reduce the

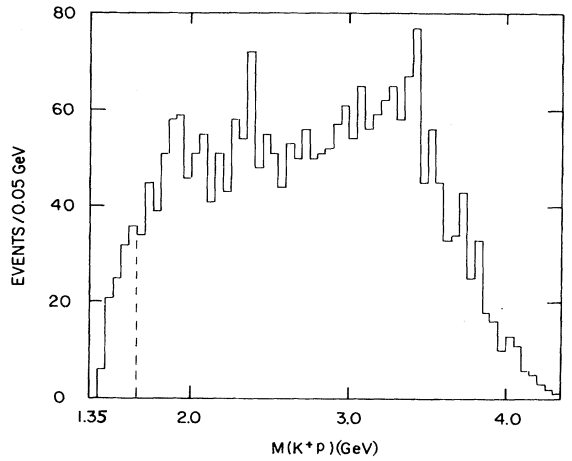

FIG. 10. $M(K^+p)$ for the reaction $\pi^+p\to K^+K^-\pi^+p$ (no Δ^{++}). The dashed line indicates the position of the cut.

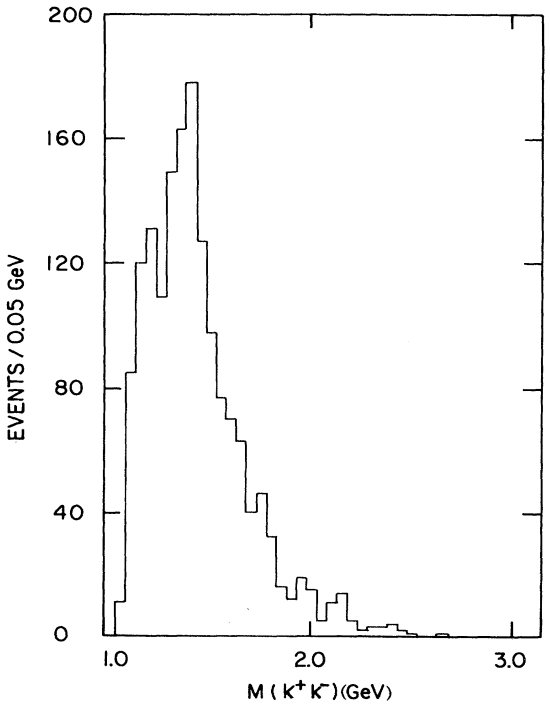

FIG. 12. $M(K^+K^-)$ for the reaction $\pi^+p\to K^+K^-\pi^+p$ (no Δ^{++}).

TABLE II. K^+K^- resonances from $\pi^+p \to K^+K^-\Delta^{++}$.

Resonance	Width Γ (MeV)	Cross section $\times$ branching ratio into K^+K^- (μb)
$f(1270)$	160±11	2.22±0.15
$g(1680)$	220±29	1.36±0.14
$h(2040)$	190±41	0.53±0.07

$\chi^2=26.0$ for 24 degrees of freedom

background due to misidentified pion and proton pairs we calculate the square of the invariant mass of the two particles forming the oppositely charged equal-mass pair $[M^2(x)]$ as described earlier. For the $K\bar{K}\Delta^{++}$ data sample we observe an enhancement around the square of the proton mass, but no indication of a pion background. We therefore require that $M^2(x)$ be less than 0.55 GeV^2, as shown in Fig. 7. Contamination from $\bar{p}p$ events is estimated to be 4%, and an upper limit on $\pi\pi$ contamination is 2%.

The events surviving the above cuts are weighted for acceptance losses as determined by a Monte Carlo simulation package. The K^+K^- mass distribution for the $K\bar{K}\Delta^{++}$ final state is shown in Fig. 8, in which a few mismeasured events with a calculated acceptance of less than 0.02 have been discarded. The solid curve on this graph represents a least-squares fit to the data of three Breit-Wigner resonance shapes plus a phase-space background. The three enhancements may be identified with the $f(1270)$, $g(1680)$, and the $h(2040)$ resonances. The results of this fit are shown in Table II. As in the neutron reaction, there is no evidence for the production of any other resonances in this case.

In order to study the virtual scattering reaction $\pi^+\pi^0 \to K^+K^-\pi^+$ we also select against the Δ^{++} region by requiring that the final-state pion have a polar angle, $\cos\theta$, with respect to the incident direction, greater than -0.7 in the center-of-mass frame, and that $M(\pi^+p)$ be greater than 1.45 GeV. In the K^-p mass distribution we again observe a low-mass enhancement due to the $\Lambda^0(1520)$ state, and remove it with the cut $M(K^-p) > 1.55$ GeV, as shown in Fig. 9. In the K^+p mass distribution we also observe a small low-mass enhancement due to a reflection of the Δ^{++} and remove this background by requiring the K^+p mass to be greater than 1.65 GeV, as shown in Fig. 10. To further reduce the background due to misidentified pion and proton pairs we calculated the square of the invariant mass of the two particles forming the oppositely charge equal-mass pair $[M^2(x)]$ as described earlier. In this case we observe no enhancements in either the proton or pion mass-squared regions, as shown in Fig. 11, and so introduced no cut on $M^2(x)$. Based on the small shoulder observed at $M^2(x) \approx 0$ we estimate an upper limit of 3% on the $\pi\pi$

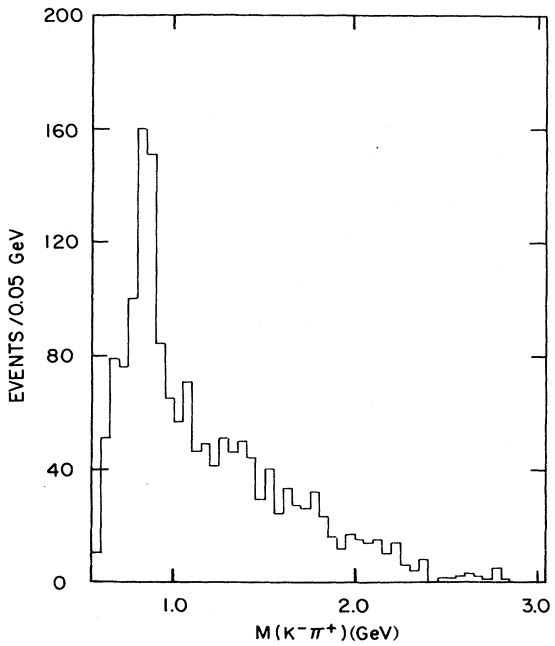

FIG. 13. $M(K^-\pi^+)$ for the reaction $\pi^+p \to K^+K^-\pi^+p$ (no Δ^{++}).

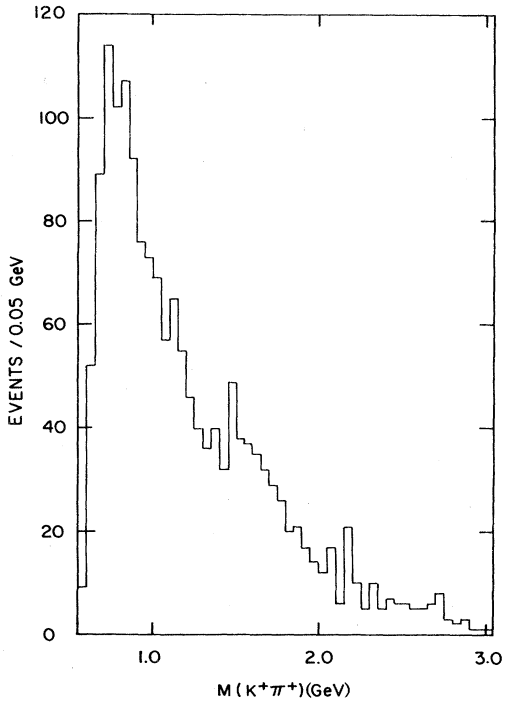

FIG. 14. $M(K^+\pi^+)$ for the reaction $\pi^+p \to K^+K^-\pi^+p$ (no Δ^{++}).

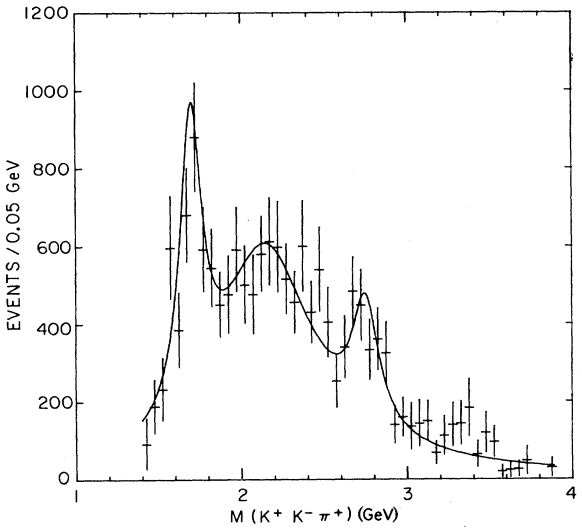

FIG. 15. Acceptance-corrected $M(K^+K^-\pi^+)$ for the reaction $\pi^+p\to K^+K^-\pi^+p$ (no Δ^{++}). The smooth curve shows the results of a fit described in the text.

contamination, but have no means to estimate possible $\bar{p}p$ background for this reaction. In Figs. 12, 13, and 14 we show the uncorrected distributions in the invariant masses of the two-body combinations $M(K^+K^-)$, $M(K^-\pi^+)$, and $M(K^+\pi^+)$, respectively. Evidence of the K^+K^- decay of the f and A_2 resonances may be seen in Fig. 12, and of the $K^-\pi^+$ decay of the $K^*(890)$ resonance may be seen in Fig. 13. As expected, the $K^+\pi^+$ mass distribution in Fig. 14 shows no particular structure.

The events surviving the cuts are weighted for acceptance losses as determined by a Monte Carlo simulation package. The $K^+K^-\pi^+$ mass distribution for the $K\bar{K}\pi p$ (Δ^{++} removed) final state is shown in Fig. 15, where events with a calculated acceptance of less than 0.02 have been discarded. The solid curve on this graph represents a least-squares fit to the data of two Breit-Wigner resonance shapes plus a background which is a representation of a Deck effect similar to that seen in 3π reactions.[13] The processes included in the Deck calculation were (a) $\pi^+p\to p\pi^+f^0$ with $f^0\to K^+K^-$, (b) $\pi^+p\to p\pi^+A_2^0$ with $A_2^0\to K^+K^-$, and (c) $\pi^+p\to pK^+\bar{K}^*(890)$ with $\bar{K}^*(890)\to K^-\pi^+$. The lower-mass enhancement may be identified with the $g(1680)$ resonance. Also in this distribution we observe an enhancement at a mass of about 2.75 GeV. The results for the fit are given in Table III.

IV. MOMENT ANALYSIS

In order to determine the spin-parity of the observed states we examine the spherical-harmonic moments of the decay-angular distributions as functions of mass. The moments presented in this paper are calculated from the acceptance-corrected data and are not the result of a fit of the spherical harmonics to the angular distribution. For this analysis, the unnormalized angular moments are calculated using the definition

$$N_i\langle Y_l^m\rangle=\sum_{j=1}^{N_i}A_i(\Omega_j,x_j)Y_l^m(\Omega_j)\ , \tag{5}$$

where N_i is the number of events in the ith mass bin, Ω_j and x_j refer to the angles and other kinematic variables for the jth event in the ith mass bin, $A_i(\Omega_j,x_j)$ is the acceptance for this event, and Y_l^m is the relevant spherical harmonic. One convenient consequence of using the angles in the Gottfried-Jackson frame is that the z component of the relative orbital angular momentum of the incident pion and the exchanged pion is zero, and since pions are spinless, the z component of the total angular momentum is also zero. In this frame, and with the assumption of pseudoscalar exchange, one expects only the Y_l^0 moments to be different from zero. The data show no significant structures in the ϕ distributions, and thus only the Y_l^0 moments are presented in this work. A resonance of mass M and spin J will appear in the first $l=2J$ moments with a peaklike structure at mass M, and will give no contribution for higher l values. In the case of a leading resonance, one expects the $l=2J$ moment to be consistent with zero for masses less than M, and the moments for $l>2J$ to be consistent with zero for masses below and through the resonance region.

The moments as functions of the K^+K^- invariant mass for the reaction $\pi^+n\to K^+K^-p$ are shown in Fig. 16. The variable used is the cosine of the angle between the incident π^+ and the K^+ in the K^+K^- rest frame, i.e., the Gottfried-Jackson angle of the K^+K^- system. The Y_0^0 moment is not shown, as it differs from the acceptance-corrected mass distribution only by a multiplicative constant. We observe evidence for two $J^P=2^+$ enhancements in the Y_2^0 moment and some indication of these signals in

TABLE III. $K^+K^-\pi^+$ resonances from $\pi^+p\to(K^+K^-\pi^+)p$.

Resonance	Width Γ (MeV)	Cross section × branching ratio into $K^+K^-\pi^+$ (μb)
$g(1680)$	160±50	0.68±0.10
$M(2750)$	195±75	0.84±0.08
	[fitted mass of $M(2750)$ is 2747±32 MeV]	

$\chi^2=34.3$ for 41 degrees of freedom

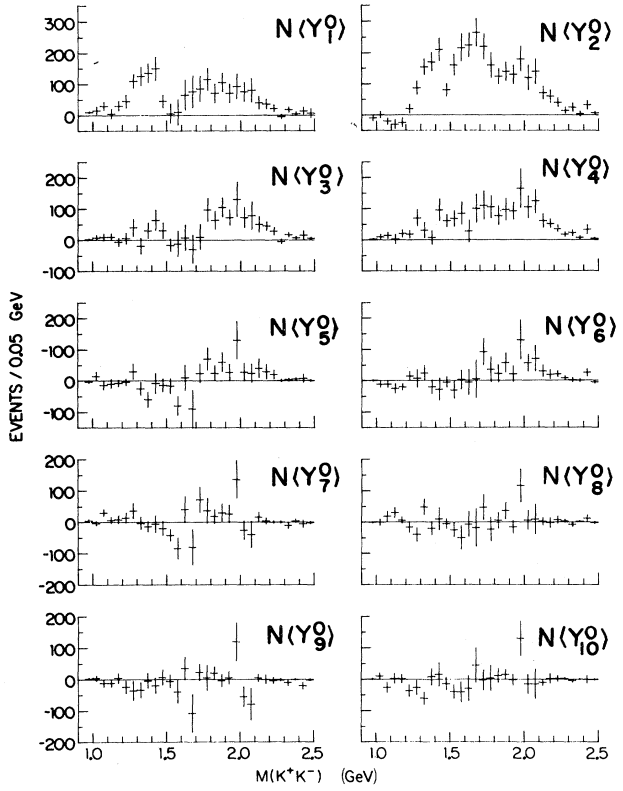

FIG. 16. Unnormalized moments of the angular distribution of the K^+ meson in the K^+K^- Gottfried-Jackson frame as a function of $M(K^+K^-)$ for the reaction $\pi^+n \to K^+K^-p$.

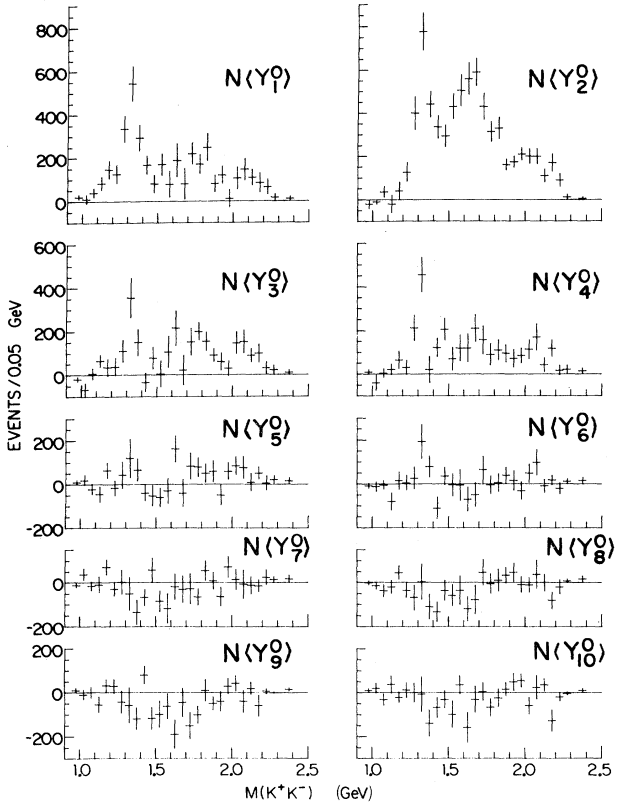

FIG. 17. Unnormalized moments of the angular distribution of the K^+ meson in the K^+K^- Gottfried-Jackson frame as a function of $M(K^+K^-)$ for the reaction $\pi^+p \to K^+K^-\Delta^{++}$.

the Y_4^0 moment. These enhancements may be identified with the $f(1270)$ and the $f'(1515)$ known resonances. We also observe a small indication of the $J^P=3^-$ $g(1680)$ meson in the Y_2^0, Y_4^0, and Y_6^0 moment distributions. The $h(2040)$ meson appears to show up most predominantly in the Y_2^0, Y_4^0, and Y_6^0 moments with only a small indication in the Y_8^0 moment.

Support for this interpretation of the moments may be found in the odd-l, $m=0$ moments, where interference effects between states of different angular momentum can be seen as a slight drop and sudden rise in the mass region between the two resonances. An example of this interference effect is seen in the mass region between the $f'(1515)$ and the $g(1680)$ resonances in the Y_3^0 moment.

The moments as a function of the K^+K^- invariant mass for the reaction $\pi^+p \to K^+K^-\Delta^{++}$ are shown in Fig. 17. The variable used here is also the Gottfried-Jackson angle of the K^+ meson. In this case there is evidence for the $f(1270)$ and $f'(1515)$ resonances in the Y_2^0 and Y_4^0 moments, which are consistent with results in the $\pi^+n \to K^+K^-p$ reaction. Also, the $g(1680)$ meson appears in the Y_2^0 and Y_4^0 moments, but is not significant in the Y_6^0 moment. The $h(2040)$ meson appears strongly in the Y_2^0, Y_4^0, and Y_6^0 moments and hardly at all in the Y_8^0 moment.

The moments as a function of the $K^+K^-\pi^+$ invariant mass for the reaction $\pi^+p \to K^+K^-\pi^+p$ (no Δ^{++}) are shown in Fig. 18. In this case the variable used is the cosine of the angle between the incident π^+ and the normal to the $K^+K^-\pi^+$ decay plane in the $K^+K^-\pi^+$ rest frame. The conservation of angular momentum, G parity, and space parity imply that for pseudoscalar exchange only states with $I=1$ and $J^P=1^-,3^-,5^-$, etc., will contribute to the $K^+K^-\pi^+$ final state. The known states that fit these criteria include the $J^P=3^-$ $g(1680)$ meson and a resonance reported by Alper *et al.*[14] with $J^P=5^-$ at a mass of 2.307 GeV. The Y_2^0 moment is consistent with a large spin-1 Deck effect similar to that seen in analyses of the reactions $\pi^\pm p \to (\pi^\pm\pi^+\pi^-)p$.[13] In the distribution of the Y_6^0 moment we observe a small peak which corresponds to the $g(1680)$ meson. However, in the distribution of the Y_{10}^0 moment we see no evidence for a $J^P=5^-$ state at a mass of about 2.3 GeV. The only indications of structure at a mass of about 2.3 GeV occur in the Y_4^0 and Y_6^0 moments. Owing to the limited statistics and large acceptance errors, the enhancement of 2.75 GeV observed in the mass distribution appears as a statistically significant effect only in the Y_{14}^0 moment. However, in each of the Y_2^0, Y_4^0, Y_6^0, and Y_{14}^0 moment distributions, some structure at a mass of about 2.75 GeV appears. The Y_5^0 and Y_9^0 moments show some indications of an interference effect in this region, but the statistical precision of these data does not permit a more sophisticated analysis. The data in the region of the 2.75-GeV enhancement are consistent with

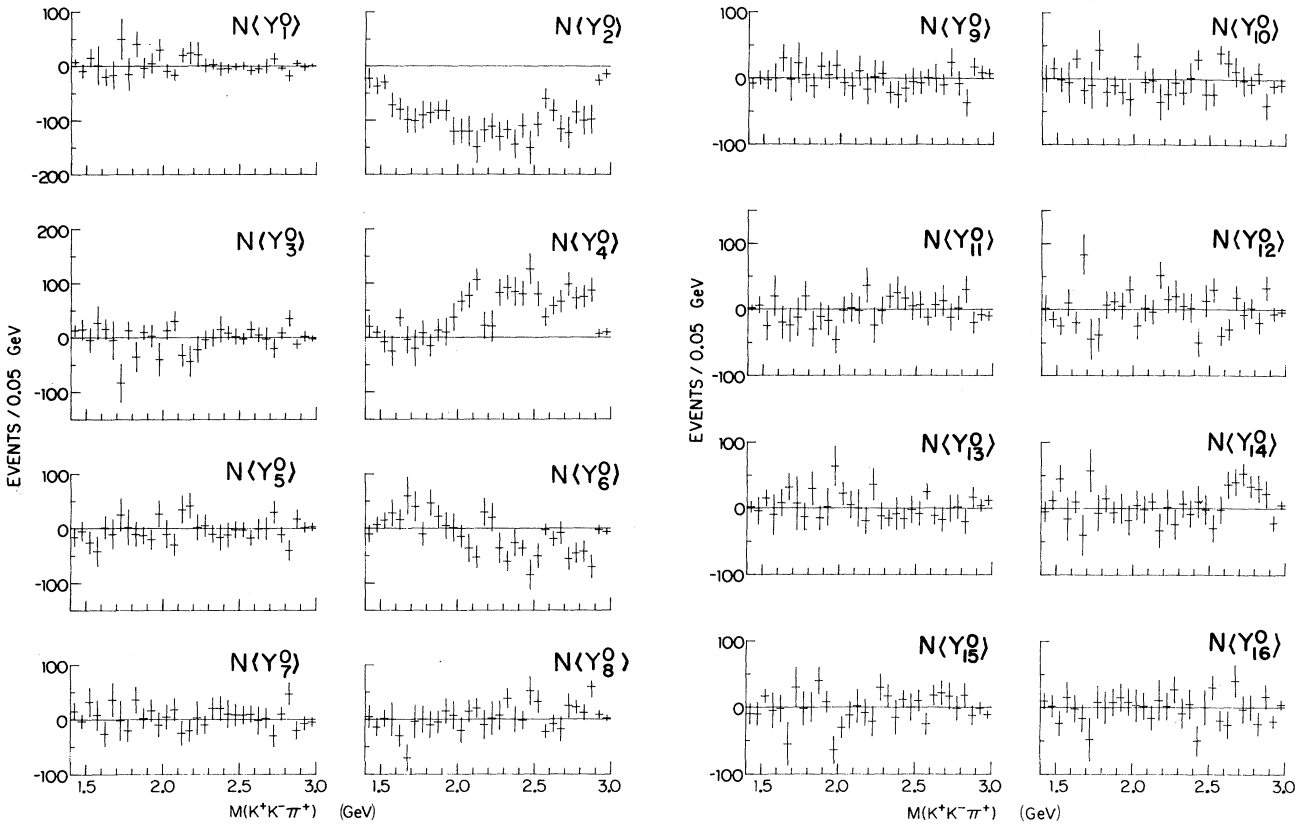

FIG. 18. Unnormalized moments of the angular distribution of the normal to the $K^+K^-\pi^+$ decay plane in the $K^+K^-\pi^+$ rest frame as a function of $M(K^+K^-\pi^+)$ for the reaction $\pi^+p\to K^+K^-\pi^+p$ (no Δ^{++}).

this enhancement being a $J^P=7^-$ object which is produced over a large spin-1 background that may be due to the large Deck amplitude mentioned earlier.

The distributions of the moments of the angular distribution for the K^+K^-p final state are consistent with those seen in previous experiments.[15–21] The distributions of the moments for the $K^+K^-\Delta^{++}$ final state are also consistent with those seen in previous experiments for $M(K^+K^-)<1.6$ GeV. Previous experiments have not explored the region with $M(K^+K^-)>1.6$ GeV in this reaction. The interpretation of the moment distributions for the $K^+K^-\pi^+p$ (no Δ^{++}) final state is consistent with the partial-wave analysis performed by G. Otter *et al.*[21] in the low-mass region below the $g(1680)$ meson. Both experiments show results which are consistent with the presence of a large, broad spin-1 Deck effect in this region. The moment analysis of the $K^+K^-\pi^+$ mass region above the $g(1680)$ meson is unique to this study.

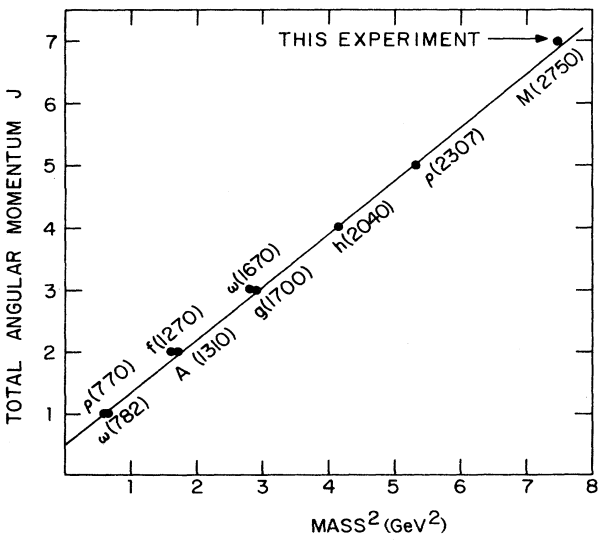

FIG. 19. Chew-Frautschi plot of the leading nonstrange mesons.

V. CONCLUSIONS

In this study, we have presented evidence for the observation of the $J^P=2^+$ resonances $f(1270)$ and $f'(1515)$, the $J^P=3^-$ resonance $g(1680)$, and the $J^P=4^+$ resonance $h(2040)$ in the K^+K^- system for the reactions $\pi^+n\to K^+K^-p$ and $\pi^+p\to K^+K^-\Delta^{++}$. We also observe evidence for the $J^P=3^-$ resonance $g(1680)$ in the $K^+K^-\pi^+$ system for the reaction $\pi^+p\to(K^+K^-\pi^+)p$. In addition, we observe evidence for a new state with a mass of 2747 ± 32 MeV and a width of 195 ± 75 MeV. The spin-parity of this new state is consistent with $J^P=7^-$, and we refer to this state as the $M(2750)$ resonance. This is the highest observed spin state for a meson resonance.

In terms of the quark model this new state would be an $I=1$ state consisting of a $u\bar{d}$ quark-antiquark pair. On a Chew-Frautschi plot (Fig. 19), the new state is seen to fall on the ρ trajectory. The $M(2750)$ resonance would be the sixth observed state on this trajectory.

ACKNOWLEDGMENTS

This work was supported by the U.S. Department of Energy, Contract No. W-7405-Eng-82, Office of Basic Science (KA-01-01), Division of High Energy and Nuclear Physics.

---

*Present address: General Dynamics Corp., Pomona, California.

†Present address: Shell Development Corp., New Orleans, Louisiana.

[1]For a discussion of one-pion-exchange reactions, see E. Ferrari and F. Selleri, Nuovo Cimento 24, 453 (1962); R. A. Leacock, *An Introduction to One-Pion Exchange Calculation in High Energy Reactions* (Institute of Atomic Research and Department of Physics, Iowa State University, Ames, Iowa, 1966).

[2]E. W. Anderson *et al.*, SLAC Proposal No. E-128, 1976 (unpublished).

[3]R. Stroynowski *et al.*, Phys. Lett. 97B, 315 (1980).

[4]F. C. Winkelman, SLAC Report No. 160, 1973 (unpublished).

[5]S. L. Shapiro *et al.*, IEEE Trans. Nucl. Sci. NS-23, 264 (1976).

[6]S. L. Shapiro *et al.*, IEEE Trans. Nucl. Sci. NS-23, 269 (1976).

[7]R. Bertolucci, Report No. SLAC-PUB-1574, 1975 (unpublished).

[8]S. Durkin, Ph.D. thesis, Stanford University, Stanford, California, 1981.

[9]A. Honma, Ph.D. thesis, Stanford University, Stanford, California, 1980.

[10]J. S. Hendrickson, Ph.D. thesis, Iowa State University, Ames, Iowa, 1981.

[11]D. L. Denney, Ph.D. thesis, Iowa State University, Ames, Iowa, 1982.

[12]J. W. Lamsa *et al.*, Phys. Rev. D 26, 1769 (1982).

[13]See, for example, G. Ascoli *et al.*, Phys. Rev. D 9, 1963 (1974).

[14]B. Alper *et al.*, Phys. Lett. 94B, 422 (1980).

[15]D. Cohen *et al.*, Phys. Rev. D 22, 2595 (1980).

[16]G. Costa *et al.*, Nucl. Phys. B175, 402 (1980).

[17]G. Grayer *et al.*, Nucl. Phys. B75, 189 (1974).

[18]A. J. Pawlicki *et al.*, Phys. Rev. D 12, 631 (1975).

[19]L. Görlich *et al.*, Nucl. Phys. B174, 16 (1980).

[20]S. D. Protopopescu *et al.*, Phys. Rev. D 7, 1279 (1973).

[21]G. Otter *et al.*, Nucl. Phys. 96B, 365 (1975).

[22]C. Evangelista *et al.*, Nucl. Phys. B154, 381 (1979).